Paper Ref: S2604_P0581
3rd International Conference on Integrity, Reliability and Failure, Porto/Portugal, 20-24 July 2009

A PARAMETRIC STUDY OF A R/C FRAME BASED ON "PUSHOVER" ANALYSIS

V.G. Pereira[1*], R.C. Barros[2], M.T. César[3]

[1] Graduate student, FEUP - Faculdade Engenharia Universidade Porto, Dept of Civil Engineering
Porto 4200-465, PORTUGAL, *Email:* ec04175@fe.up.pt
[2] Prof. of Civil Engineering, FEUP - Faculdade Engenharia Universidade Porto
Dept of Civil Engineering, Porto 4200-465, PORTUGAL, *Email:* rcb@fe.up.pt
[3] Assistant Lecturer, IPB-Instituto Politécnico Bragança, Dept of Applied Mechanics
Bragança 5301-857, PORTUGAL, *Email:* brazcesar@ipb.pt

SYNOPSIS

Three commercial software packages (SAP 2000, SeismoStruck and MIDAS/CIVIL) universally used in the design of civil engineering structures, are applied on a parametric study of pushover analyses of a RC frame of an office building under a few evaluative phases. In order to represent the influence of the masonry infill panels the equivalent tie method is used; for a sensitivity study on the capacity curves, several values for the tie width are considered. The comprehensive parametric study also addresses the influence of other parameters, on the structural behavior and non linear capacity curves of the RC frame, namely: length and location of the plastic hinges forming near the end of the structural elements, and different loading patterns (with uniform, modal and triangular distributions).

NON-LINEAR STATIC ANALYSIS

In the design of structures under seismic actions several methodologies can be used, with distinct accuracy, to describe the structural seismic response. The non-linear dynamic analysis is the most realistic methodology and is based on the timely variation of the structural behavior of the materials and of the geometry, including material and geometric nonlinearities, under seismic actions. Although this methodology is the most accurate, its non-linear characteristics require knowledge of the structural behavior and inherent theoretical developments and it also demands costly computational resources. Such conditions are not often timely compatible with the design procedure besides the fact that most of the design does not justify the application of such elaborated models.

However, the design engineers need intuitive tools to determine the structural response under seismic actions, in particular for those that are strongly conditioned by dynamic actions. In this sense, several researchers try to develop simplified analysis and design methodologies based on non-linear analysis, for the determination of the structural response and that can be routinely used by the structural designers.

Concisely, the methodologies for analysis of buildings under seismic actions can be divided in linear procedures and non-linear procedures. The last procedures include the non-linear static procedure and the non-linear dynamic procedure. When the structures present strong irregularities or when the response occurs significantly in the non-linear domain, non-linear analysis should be used. The non-linear static procedure was initially applied to structures that did not present great sensibility for higher modes of vibration. Despite the fact that the dynamic behavior of most structures is dominated by the first mode of vibration, this behavior cannot be generalized to all kind of structures.

Other limitation to this methodology is the fact that the progressive degradation of the stiffness that occurs during the nonlinear cycling load of the seismic actions is not considered. This degradation has great consequences on the structural response, such as modification of the modal characteristics and rising the period of the structure.

The recent advent of performance based design has brought the nonlinear static pushover analysis procedure to the forefront. Pushover analysis is a static, nonlinear procedure in which the magnitude of the structural loading is incrementally increased in accordance with a certain predefined pattern. With the increase in the magnitude of the loading, weak links and failure modes of the structure are found. The loading is monotonic, with the effects of the cyclic behavior and load reversals being estimated by using a modified monotonic force-deformation criteria and with damping approximations. In other words, local nonlinear effects, such as flexural hinges at the member joints, are modeled and the structure is deformed or "pushed" until enough hinges form to develop a collapse mechanism or until the plastic deformation limit of a certain hinge is reached.

For the case of a building with applied horizontal actions, such as seismic actions, the nonlinear flexural deformations occur near the elements extremities. The elements can be idealized admitting that the nonlinear behavior is described as inelastic deformations lumped in certain extensions with fixed lengths near the extremities. In another way, it can also be considered that the distribution of the inelastic deformations occurs along a certain specific length of the element.

In order to avoid all the limitations of this nonlinear static procedure, some analysis methods have been proposed. One of them, quite simple and applicable to structures with multiple degrees of freedom, has been proposed by Fajfar and Fischinger [1]. This method, known as N2-method, is actually presented in Eurocode 8 (EC8) [2] and is correctly developed in the next chapter of this paper.

Nowadays the static non-linear analysis is considered as a valid alternative to the dynamic nonlinear analysis, in order to verify the structural safety of RC frames, under seismic actions. Nevertheless this consideration cannot be generalized for all types of structures, and it is always necessary to know all the limitations and potentialities of the methodologies.

PUSHOVER ANALYSIS (Method N2)

The N2 method was originally developed in 1988 by Fajfar and Fischinger [1] and it is the adopted method in recent versions of Eurocode 8 (EC8) [2]. In the next paragraphs the method is fully described, as it appears in the regulation above-mentioned and as utilized by Cesar and Barros [3] [4] in a parametric study of multi-storey steel buildings.

Firstly, the structural elements must be modeled attending to their physical nonlinearities, implementing the constitutive nonlinear relationships for the different kind of structural elements.

In the case of EC8, the proposed methodology is based on an elastic spectrum representation that presents the spectral values of the acceleration in function of the spectral values of the displacement; in other words, it is presented in the format Acceleration Displacement Response Spectrum (ADRS).

For a single degree of freedom (SDOF) with natural period T and elastic behavior, equation (1) is valid in which S_e and S_{de} represent, respectively, the elastic spectral response of the acceleration and of the displacement.

$$S_e = \frac{4 \cdot \pi^2}{T^2} \cdot S_{de} \tag{1}$$

Next, the capacity curves of the structure must be obtained, which bring into relation the base shear F_b with the control node displacement of the structure d_n (which quite often corresponds to the top). As demanded in EC8, the capacity curve should be obtained until the top displacement reaches 150% of the target displacement. The loading pattern should contemplate at least two distributions, modal and uniform.

Because the elastic spectrum of the seismic action is given for a single degree of freedom (SDOF), it is necessary to transform the capacity curves of multiple degrees of freedom (MDOF) into a system of only one single degree of freedom. The current transformation is done by the transformation factor Γ, shown below in equation (2), where Φ_i is the modal component associated to the floor i and m_i is the mass associated to the floor i.

$$\Gamma = \frac{\sum m_i \phi_i}{\sum m_i \phi_i^2} = \frac{m^*}{\sum m_i \phi_i^2} \tag{2}$$

The transformation, to convert the capacity curves for an equivalent SDOF, is done through the following relationship:

$$F^* = \frac{F_b}{\Gamma} \tag{3}$$

$$d^* = \frac{d_n}{\Gamma} \tag{4}$$

After all the steps done before, it is necessary to simplify the capacity curve for an elastic-perfectly plastic regime (Figure 1). In this graph, F_y^* represents the resistant strength capacity of the system with an equivalent SDOF and d_y^* represents the idealized yield displacement of the equivalent SDOF system. The yield displacement is given by equation (5), where E_m^* is the deformation energy until the plastic hinge is formed and d_m^* is the displacement for that point. The initial stiffness of the idealized system is determined in such a way that the areas under the actual and the idealized force-deformation curves are equal.

$$d_y^* = 2 \cdot \left(d_m^* - \frac{E_m^*}{F_y^*} \right) \tag{5}$$

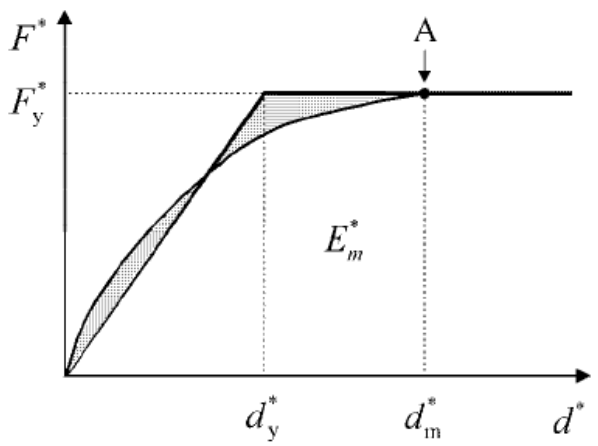

Figure 1 – Idealization of the capacity curve (Eurocode 8)

The period idealized for an equivalent SDOF system is determined by:

$$T^* = 2\pi \cdot \sqrt{\frac{m^* \cdot d_y^*}{F_y^*}} \tag{6}$$

The target displacement of the structure with period T^* and unlimited elastic behavior is given by equation (7), where $S_e(T^*)$ is the elastic acceleration response spectrum at the period T^*.

$$d_{et}^* = S_e(T^*) \cdot \left[\frac{T^*}{2\pi}\right]^2 \tag{7}$$

The equivalent system does not present an unlimited elastic behavior, so the target displacement (known as d_t^*) may not be equal to d_{et}^* because it depends on the dynamic characteristics of the equivalent SDOF system.

Figures 2 and 3 illustrate how to determine the target displacement. In this figures, it is showed the response spectrum in ADRS format, and also the capacity curve idealized for a SDOF system. What separates the short periods from the medium and long periods is the period T_c, which is the characteristic period associate to the soil movement.

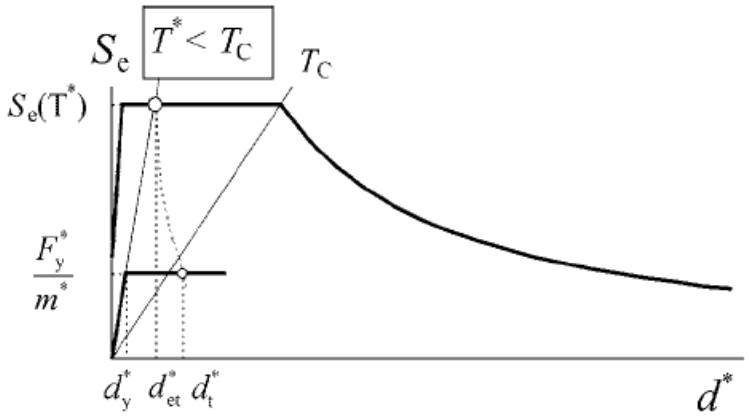

Figure 2 – Short period range

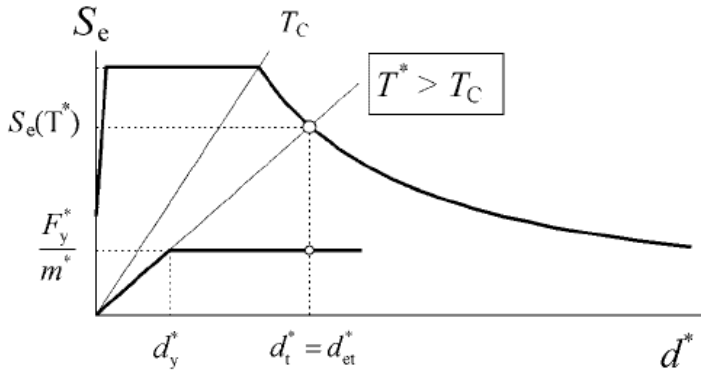

Figure 3 – Medium and long period range

For short period range $T^* < T_c$ and if the structure presents elastic behavior ($F_y^*/m^* > S_e(T^*)$), the value of d_t^* is given by equation (8).

$$d_t^* = d_{et}^* \tag{8}$$

In case the structure presents an inelastic behavior ($F_y^*/m^* < S_e(T^*)$) the value of d_t^* is now given by equation (9); the parameter q_u represents the reduction factor associate to the dissipated energy (very often in ductile structures) and is calculated by equation (10).

$$d_t^* = \frac{d_{et}^*}{q_u} \cdot \left(1 + (q_u - 1) \cdot \frac{T_c}{T^*}\right) \geq d_{et}^* \tag{9}$$

$$q_u = \frac{S_e(T^*) \cdot m^*}{F_y^*} \tag{10}$$

For medium and long period range, $T^* > T_c$, the same equality is assumed as in equation (8).

The value of the target displacement for a SDOF system is obtained intersecting the first segment of the bi-linear capacity curve with the descending branch of the graph of the elastic ADRS response spectrum (S_a vs S_d).

In order to determinate the target displacement for the MDOF system, it is finally necessary to obtain the top displacement of the structure, through the equation (11).

$$d_t = \Gamma \cdot d_t^* \tag{11}$$

This displacement corresponds to the control node, which should be applied to the mass center of the structure top floor. Considering the new capacity curves obtained with this top displacement, the rotations displacements and drifts can be determined, with which the structural safety of the RC frames and the damage under seismic actions can be verified.

CONSIDERATIONS ON PLASTIC HINGES FOR PARAMETRIC STUDIES

In the implementation of pushover analysis, modeling is one of the important steps. The model must consider nonlinear behavior of structure and so of its elements. Such a model requires the determination of the nonlinear properties of each component in the structure, which are quantified by strength and deformation capacities. In this paper, all plastic hinge aspects are approached as considered relevant to the analysis. The three software to be used in the pushover analyses are: SAP 2000 [5], MIDAS/CIVL [6] and SeismoStruck [7].

Modeling with Concentrated Nonlinearity

Lumped plasticity is a commonly used approach in models for deformation capacity estimates. The ultimate deformation capacity of a component depends on the ultimate curvature and plastic hinge length. The use of different criteria for the ultimate curvature and different plastic hinge length may result in different deformation capacities. Several plastic hinge lengths have been proposed in the literature. Also the type of plastic hinge is described in this chapter. For the pushover analyses realized with concentrated hinges, SAP 2000 [5] and MIDAS/CIVIL [6] are in fact the two commercial software used to reach such goal.

Plastic Hinge Length

Using SAP 2000 [5] some authors have proposed various expressions in order to establish the correct hinge length. Park and Paulay [8] presented the following expression, in which L_p is the plastic hinge length and h is the section height:

$$L_p = 0{,}5 \times h \tag{12}$$

A group of Canterbury University, studying the problematical definition and quantification of the hinge length, admitted latter a bilinear approximation to the relation moment-curvature. The curvature distribution admitted corresponds to an elastic-plastic approximation for the relation moment-curvature in the reinforced concrete sections, and a zone with plastic deformation where the plastic curvature is constant. Based on the results obtained, Park Priestley and Gill [9] proposed the expression of equation (13) in order to calculate de plastic hinge length, where l is the element member length and d_b is the diameter of the reinforcement steel bars.

$$L_p = 0{,}08 \cdot l + 6 \cdot d_b \tag{13}$$

More recently, Priestley Seible and Calvi [10] proposed again a new expression for the hinge length in which they have considered that not only the distance from the critical section to the point of null bending moment influences the value of the length but also the yield strength can generally influence.

The expression is given by equation (14), where f_{ye} is the yield strength of the longitudinal bars and l_c is the distance between the plastic hinge and the null bending moment of the element.

$$L_p = 0{,}08 \cdot l_c + 0{,}022 \cdot f_{ye} \cdot d_b \geq 0{,}044 \cdot f_{ye} \cdot d_b \tag{14}$$

Using the software MIDAS/CIVL [6], the plastic hinge length always assumes a constant value which is automatically defined by the program.

Localizing the Plastic Hinges

It is commonly known that the adequate locations where the plastic hinges are formed, in RC frames submitted to bending forces, are in fact the extremities of the elements. In frames that constitute a certain building, generally is on the extremities of beams and columns that the cracking process takes place: in those locations the bending moments are more intense and as consequence, those are the sections where the nonlinear deformations exists because of the inelastic behavior of the materials.

It is possible to verify that it is necessary a higher number of plastic hinges in order to form a collapse mechanism, if they are formed on the beams extremities. If the hinges are formed on the extremities of all columns at the same storey, the load cannot rise and plasticity cannot evolve along the structure. It can also be observed that columns have less available ductility and the formation of plastic hinges in these elements involves a significant increase of the P-delta effects, which in turn can precipitate or induce collapse.

So, in what refers to the location of the plastic hinges when using the software SAP 2000 [5] and MIDAS/CIVIL [6], one case is studied: the introduction of the plastic hinges near the end of the structural elements, with a certain distance away from the extremity of the element. If using SAP 2000 [5] in the analysis, the distance between the concentrated hinge and the extremity of the element is half the length of the hinge. If using MIDAS/CIVIL [6] the program automatically introduces the hinge at a distance d of the extremity, where d is the height of the element section.

Types of Plastic Hinge

For the columns that compose the frame, it is necessary to take into account the interaction between the axial force and the bending moments (P-My-Mz), therefore being fundamental obtaining the interaction curves. To achieve that goal the program FAGUS [11] was used, since it constitutes most of the times the elected one in the most prestigious design offices dealing with the design of RC frames. In this work the program was used with special permission of AFA – Consultores de Engenharia Lda, a fact that is herein acknowledged.

When analyzing beams, they are simulated with the exclusive contribution of the bending moments (My-Mz); so in such case it is not necessary to obtain the interaction curves because the axial force is neglected. Finally, the masonry walls are simulated considering only the axial force (P); this is so because in all the three software the masonry filled panels are simulated with the introduction of equivalent ties, which exist only in compression.

Modeling with Distributed Nonlinearity

Intending to model RC frame pushover with distributed nonlinearity, the program SeismoStruck [7] has appropriate features. It uses a tridimensional fiber model based on finite elements, and all the analyses are treated as potentially nonlinear considering material and geometric nonlinearity. The distribution of inelasticity along the length of the elements is modeled through a cubic approximation that allows a precise estimative of the damages. The tension-extension state of the elemental sections is obtained integrating the individual nonlinear and uniaxial response of each fiber in which the section of the member element was divided. In order to integrate the equations of the cubic interpolation functions that govern the nonlinear response, two Gauss points per element are used.

CONSIDERATIONS FOR THE PUSHOVER ANALYSES OF A R/C FRAME

Introduction to the Structure under Study

In this work, one of the main goals to achieve is obtaining the capacity curves of a reinforced concrete frame, constituted by two storey’s and two bays, of an office building situated in Lisbon area. It will be realized as a parametric study, with bay widths of 5-6-7 meters and story heights of 3-3.5-4 meters respectively. The three software presented before -- SAP 2000 [5], MIDAS/CIVIL [6] and SeismoStruck [7] -- are the chosen ones, in order to develop the pushover analyses of the RC frame.

In this work it is also addressed the influence of the masonry infill, i.e. of the masonry filled panels in the building. The influence of other parameters on the structural behavior of the RC frames is also presented. Those parameters are defined to be the length and location of the plastic hinges (Park and Paulay [8], Park et al. [9], Priestley et al [10]) forming near the end of the structural elements, because bending moment is the predominant generalized force in the structure. Finally, it is also important to see the non linear material behavior of the structure when submitted to different load patterns, such as: uniform, modal and triangular.

The RC frame geometry is presented in general form in Figure 4. During the pushover parametric analyses of the frames they will be considered to go through diverse steps or phases, since the general frames can be irregular in plan and in elevation, because for RC frames under seismic actions the sequence of damages is often dependent on such irregularities. The effect of irregularities was then assessed by the evaluative steps in Figure 5.

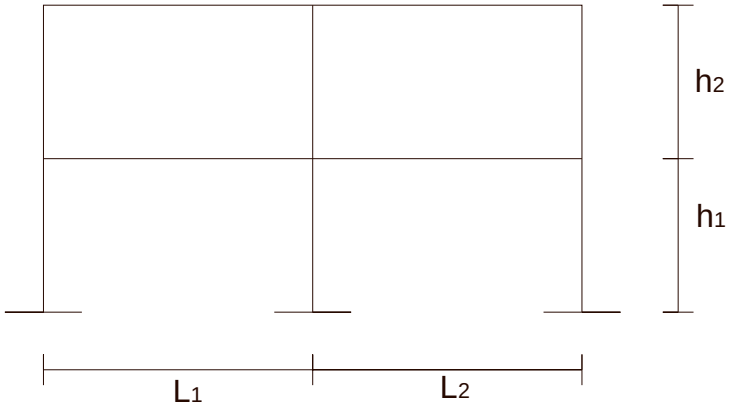

Figure 4 – Vertical elevation view of the RC frame

Therefore the current static nonlinear procedure of the proposed frames is based in four evaluative steps, which are shown in Figure 5. In what refers to the sections of the RC members, they are constituted by concrete C30/37 and steel S500.

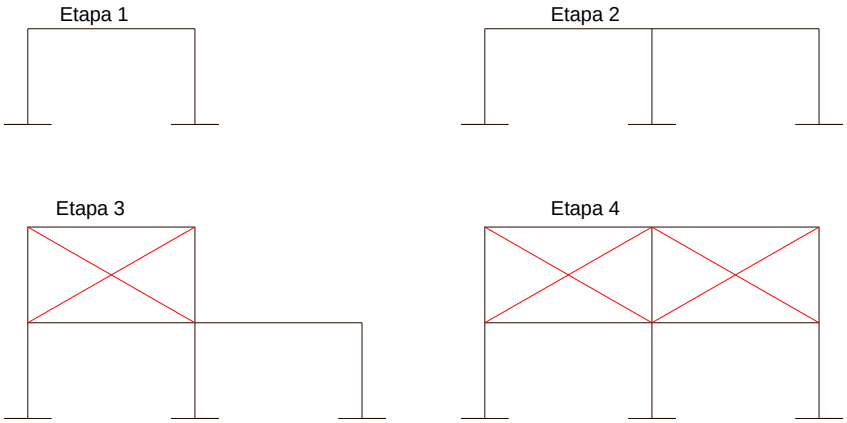

Figure 5 – Pushover analysis evaluative steps

Finally, the design of all RC members was done with help of SAP 2000 [5] based on Eurocode 2 (EC2) [12], with which all the longitudinal and transversal reinforcement bars were obtained. In order to calculate them, the following actions were assumed: wind, seismic actions, permanent and live loads. When analyzing all possible combinations it has been given special emphasis to the last case of the parametric study, because it is the most significant with respect to the structural member forces.

In the determination of the transversal sections of the elements, the concrete sections were initially admitted, for beams and columns, respectively:

- Superior beams: 0,2 x 0,5 m^2
- Inferior beams: 0,3 x 0,6 m^2
- columns: 0,3 x 0,3 m^2

In Figure 6 are identified all the structural elements, in order to easily associate them to their corresponding RC transversal sections (Figures 7 through 11).

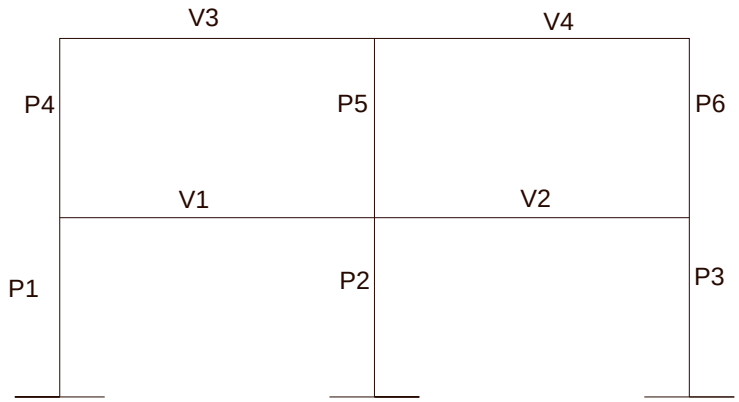

Figure 6 – Identification of the RC frame structural elements

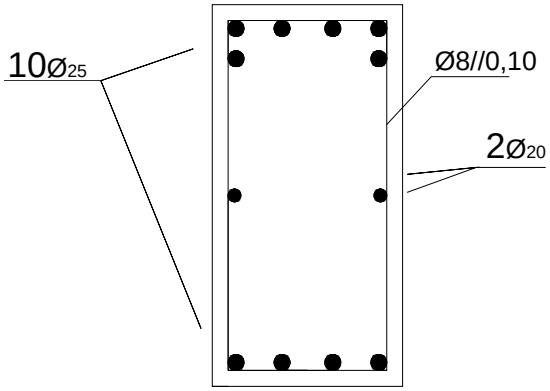

Figure 7 – RC section for beams V1 and V2

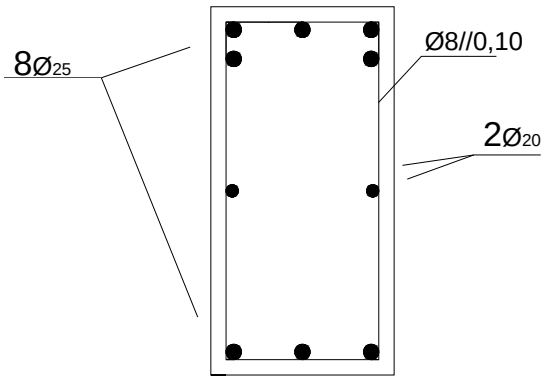

Figure 8 – RC section for beams V3 and V4

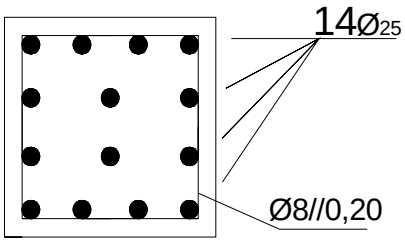

Figure 9 –RC section for columns P1-P3-P4-P6

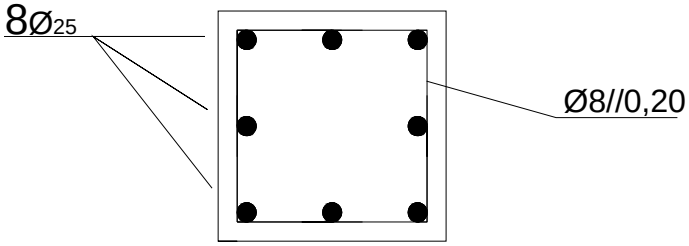

Figure 10 – RC section for column P2

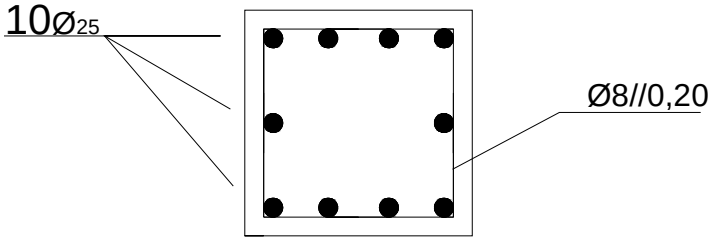

Figure 11 – RC section for column P5

Load Pattern Adopted

To evaluate the seismic performance of the structure, the choice over the possible load patterns is very important in order to correctly develop each pushover analysis of the parametric study. The load pattern is intended to represent the distributions of inertia forces resultant of seismic actions.

In this very paper it will be adopted the two distributions presented in EC8 [2], which are the uniform and the modal distributions. These distributions are based on proportionality to masses and to the product between masses and modal displacements, respectively. There is also the triangular distribution, in which the forces are proportional to the story elevation.

Masonry Infill Panels

Due to introduction of new materials for building frames, such as the steel and the concrete, the use of the masonry walls as structural elements is reduced and they are used essentially as decoration or partitioning. Because of that, their participation in the buildings structural behavior is commonly neglected in the design phases.

In what refers to geometry and mass, the plan and elevation irregularities can cause unwanted problems over the structures; many damages and collapses have been caused in so many irregular structures for recent seismic events. Those irregularities can origin horizontal forces redistributions and deformations very different from those in regular structures (Moehle and Mahin [13], Barros and Almeida [14]).

It is commonly seen in reinforced concrete buildings that masonry walls do not exist in lower storey's, due to architectonic reasons or functional reasons or others such as space occupation. In this way those options have been leading to frequent collapse of (regular and irregular) buildings, because of created soft-storey mechanisms.

PERFORMANCE OF MASONRY-FILLED R/C FRAME BUILDINGS

The type of failure that will occur in a masonry filled frame is normally difficult to predict, depending on several factors such as: the relative stiffness of the frame and the infill panel, the strength of their components and the dimensions of the structure. The collapse of the system involves one or more simple types of failure, which can occur in the masonry infill as well as in the frame. Describing these modes of failure is the main objective of this section.

The different mechanisms of failure affecting the components of the filled frames are defined, in a general sense, as modes of failure. In some cases, however, the local failure of one component does not represent the failure of the whole system and should be regarded only as a serviceability limit state. The figures presented in the following sections illustrate separately these mechanisms for sake of clarity. The final failure of the filled frame usually results from a combination of them. The failure of the masonry panel can be developed by de-bonding of the mortar joints, cracking or crushing of the masonry units or a combination of these. The occurrence of the different types of failure depends on the material properties and on the stress state induced in the panel.

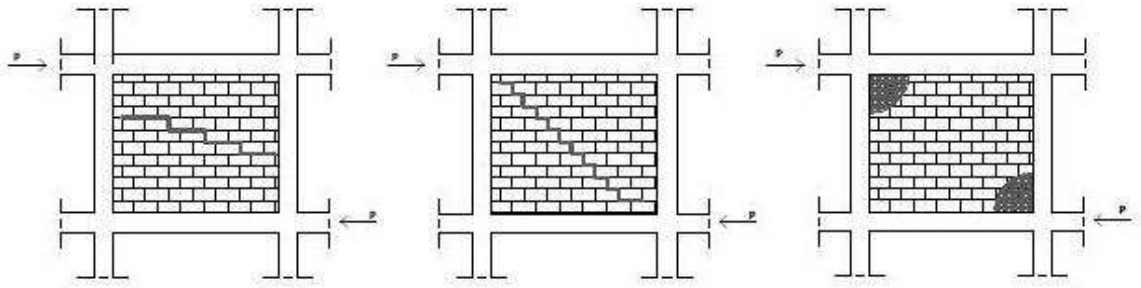

Figure 12 – Modes of failure of masonry walls

Shear cracking

Cracking in masonry panels due to shear stresses is the most common type of failure observed in the experimental work an also in masonry filled frame buildings affected by earthquakes. This type of failure is mainly controlled by the shear strength of the mortar joints (bond strength and coefficient of friction), the tensile strength of the masonry units and the relative values of the shear and normal stresses. Depending on these parameters, the combination of shear stresses with vertical axial stresses can produce either cracks crossing the masonry units or de-bonding along the mortar joints (also termed as shear friction failure).

i) Stepped Cracking Along the Mortar Joints

When the mortar joints are weak in comparison with the masonry units or when the shear stress predominates over the normal stress, cracking usually occurs by de-bonding along the mortar joints. This mode of cracking has been widely observed in laboratory tests, as well as in masonry filled frame buildings subjected to earthquakes, and it can be regarded as the most common type of failure.

ii) Horizontal Sliding Along the Mortar Joints

It has also been observed a different mechanism, in which the panel fails by sliding shear due to the formation of a horizontal crack. This type of failure was reported by several researchers, in testes of masonry filled reinforced concrete frames. Tests results indicate that the major crack usually starts a few courses below of the upper loaded corner and continues diagonally downwards to approximately the centre of the panel. The cracks propagate horizontally. When the direction of the force is reversed, the horizontal crack increases its length, crossing the panel.

iii) Cracking Due to Diagonal Tension

The stress induced in the masonry by the lateral forces can produce diagonal cracks which occur because the stress state exceeds the tensile strength of the masonry unit. These cracks start in the central zone of the panel, where the tensile principal stresses are higher, and then propagate towards the corners, running with a certain inclination. This type of cracking usually occurs when the mortar joints are strong in comparison with the masonry units or when the normal stress predominates over the shear stress. The distribution of the diagonal cracks depends on the characteristics of the masonry wall and the panel-frame interface. When the panel is horizontally reinforced or when the conditions of the panel-frame interfaces are improved, as occur in framed masonry, the cracks are usually small and distributed in a wide zone along the diagonal. In other cases, the damage concentrates in one or two large cracks. However, this is not a general conclusion and it is difficult to predict the cracking pattern for a particular case.

Compressive failure

Failure of the masonry due to compression has been observed following two mechanisms, resulting of the different stress states which develop in the infill panel at the loaded corners and along the diagonal.

i) Crushing of the Loaded Corners

The first mechanism of compressive failure can occur in the regions close to the loaded corners, where a biaxial compression-compression stress state develops due to the lateral loading. The biaxial stress regimen improves the strength of the masonry; however, the values of the stress are higher in these zones.

ii) Compressive Failure of the Diagonal Strut

This mechanism is associated with diagonal cracking. After the cracks occur, the tensile strength along the diagonal are relieved and the masonry between the cracks behaves like small prisms axially loaded. As a result of the increase of the lateral displacement, the separation of the cracks grows leading to a failure of the panel by instability of the cracked masonry. Therefore, this type of failure occurs as a consequence of diagonal tension cracking. In infill panels built with hollow masonry units, a sudden compressive failure is prone to occur after cracking because this type of masonry units is normally made of brittle, high-strength materials to compensate the large area of voids.

Flexural Cracking

In those cases where effects are predominating and the columns of the frame are very weak, flexural cracks can open in the tensile side of the panel due to the low tensile strength of the masonry.

Modeling of the Masonry Infill Panels in the Software

The first publication about the masonry infill walls participation in RC frames submitted to horizontal loads appears to be made Polyakov [15] in 1956, in which tests were realized in order to study the influence of various types of masonry, varying parameters such as: number of blocks, type of mortars used in the joints, type of load (monotonic and cyclic) and the effect of the openings.

Observing those testes Polyakov [15] introduced the new concept of equivalent tie, noticing that the frames filled with masonry start to have a monolithic behavior until the separation of blocks is reached except small regions that maintain the contact in the corners. Then the masonry panels start to function as ties only under compression, with simultaneous appearing of cracking in those directions.

Polyakov [15] concluded that the wall-frame structural set has a monolithic behavior for lower horizontal loads; but if the loads increase their intensity, the lateral deformation rises too and the wall-frame behavior becomes more complex, with separation between the frame and the masonry panel. In that situation, the frame suffers bending deformations and the masonry panel suffers shear deformation, remaining only the contact in the compressed corners. This type of behavior can significantly change if there is any kind of link between the frame and the panel.

In fact it is possible to simulate (in a simplified way) the participation of the masonry infill panel, over the global structural response, using diagonal ties (Figure 13); such ties should have the mechanical and geometric characteristics that reproduce the behavior of the wall and of the wall-frame structural set.

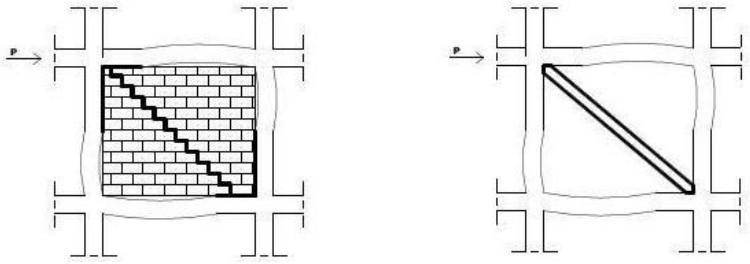

Figure 13 – Equivalent diagonal tie

The mechanical and geometric characteristics of these ties are absolutely a preponderant factor (Stafford Smith and Carter [16]), because through experimental observations, it was concluded that stiffness and the diagonal resistance of the walls do not depend on their dimension and physical characteristics; they depend on the contact length between the wall and the frame.

Other authors proposed some empirical and also conservative formulas with the intention to determine the equivalent width *w* of the ties. Riddington and Stafford Smith [17] as well as Paulay and Priestley [18], proposed: $w = 0{,}10\ d$ and $w = 0{,}25\ d$, in which *d* is the diagonal length of the tie. In this way Table 1 presents all the fundamental aspects relevant to the equivalent ties, considering the two joint proposals before-mentioned.

Table 1 – Fundamental aspects related to the equivalent ties

Cases	d (m)	w (m)	t (m)
1	5,434	0,543 1,359	0,25
2	6,552	0,655 1,638	0,25
3	7,670	0,767 1,918	0,25

The adopted masonry wall in this paper is presented in Figure 14. In what refers to the mechanical values of the wall, the Young modulus is considered as 6 GPa and the panel has a self weight of about 2,2 kN/m^2. It is constituted by brick blocs with dimensions 30x20x7 cm^3.

In what refers to the masonry infill panels behavioral models, using SeismoStruck [7], two models were conveniently selected from all the possible models presented in the program: “Masonry infill strut curve” (Inf_strut) and “Masonry infill shear curve” (Inf_Shear). Both models were developed and initially programmed by Crisafulli [19], and were introduced later in the program by Blandon [20].

Due to difficulties developing a general model that could cover all the potential modes of failure described, only some of them were considered; such is the case of cracking associated to shear and compressive failure of the equivalent ties.

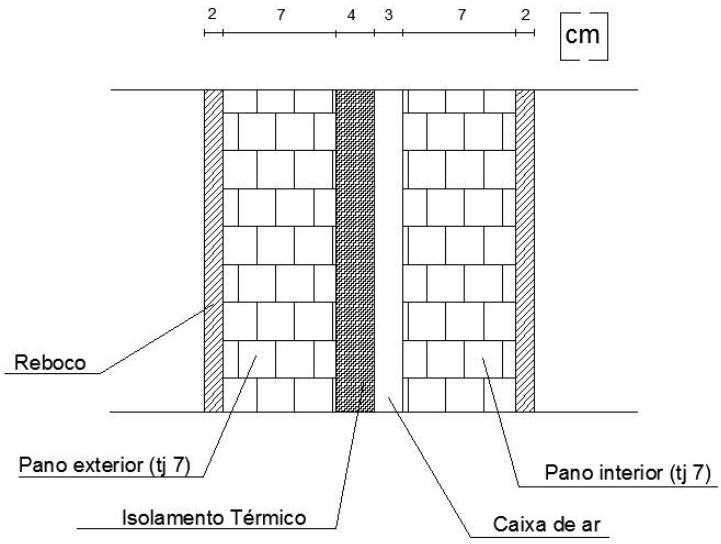

Figure 14 – Section of the masonry wall in a plane perpendicular to the RC plane frame

The curves that represent those behaviors are exposed below (Figures 15 through 18) and all their content is now conveniently described and justified.

Unloading and reloading is a complex phenomenon that is very difficult to be modeled accurately. Generally, the approach adopted by Crisafulli [19] is based on an analytical model that uses a curve which passes through two predefined points (Figure 15), where the slope of the curve is known. A nonlinear continuous expression is proposed to represent the unloading-reloading curves, the main advantage of which is that the slope of the curve can be imposed at both ends.

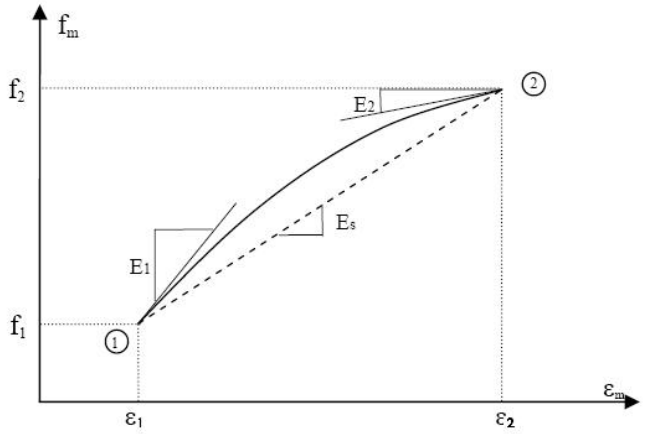

Figure 15 – Proposed curve for unloading and reloading

Experimental results indicate that the unloading curves exhibit a simple curvature and have shapes dependent on the level of unloading strain. The unloading curve (rule 2), as it is shown in Figure 16, starts from the envelope curve (ε_{un}, f_{un} – rule 1) and finishes with a residual or plastic deformation ε_{pl}, which seems to be the most important parameter in determining the unloading curve. For the prediction of the value of ε_{pl}, empirical expressions have been proposed but with limited validity. Crisafulli [19] expanded a general approach used earlier, introducing an empirical constant in the calculation of ε_{pl}.

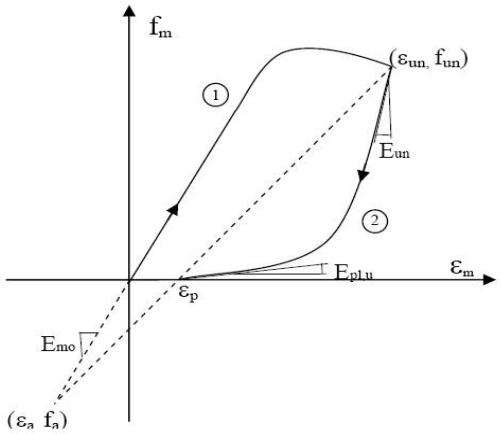

Figure 16 – Stress-strain curves for unloading branch

Figure 17 shows the reloading and unloading paths and the parameters that define such curves. The unloading curve starts when the compressive strain ε_m reaches the plastic strain ε_{pl}. After that point the compression stress increases following a path different from the one corresponding to unloading. The shape of the reloading curve is complex, showing double curvature with mild concavity in the low stress region and a sharp reversal in curvature near the envelope. The reloading curve consists of two curves. The first one (rule 4) goes from the point reloading (ε_{pl}, 0) to an intermediate point (ε_{ch}, f_{ch}). Then the second curve (rule 5) continues until the envelope curve is reached. The modulus used as final for rule 4 is used as initial for rule 5, assuring continuity. The resultant curve and its derivative are continuous, representing thus successfully the changes of curvature observed in tests of masonry.

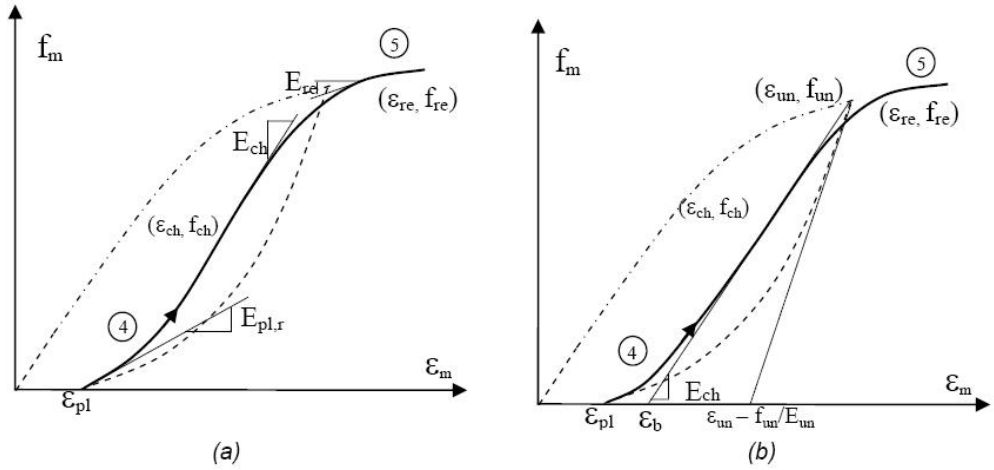

Figure 17 – (a) Reloading curve and associated parameters; (b) Definition of change point for unloading curve

The rules previously described define the loops that start from and return to the envelope curve with only one reversal after complete unloading. But reversals can happen at any place during the loading history. For the sake of completeness, the model proposed by Crisafulli [19] includes the effect of the inner loops.

Because of the complexity of the behavior and of lack of data, Crisafulli [19] conducted tests on standard concrete cylinders with different combinations of complete and inner loops. The conclusions drawn were: (i) the successive inner loops increase the reloading strain; (ii) the inner loops do not affect the plastic deformation; (iii) the inner loops remain inside the cycle defined for the complete unloading and reloading curves.

The former can exhibit change in direction of its concavity depending on the starting point of the loading curve, while the latter show no inflection point. A typical cyclic response with small cycle hysteresis is represented in Figure 18.

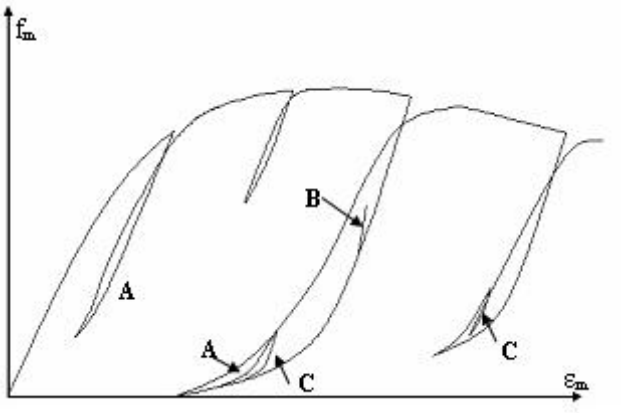

Figure 18 – Typical cyclic response with small cycle hysteresis

In what refers to the shear model, the adopted model is capable of representing the shear behavior when bond failure happens along the mortar joints. It is assumed that the behavior of the latter is linear elastic while the shear strength is not reached. Unloading and reloading are also in the elastic range. Thus, the shear stress τ is equal to the shear deformation γ times the shear modulus G_m.

The model consists of two simple rules and includes the axial load in the masonry as a variable in the shear strength. The shear strength is evaluated following a bond-friction mechanism, consisting of a frictional component and the bond strength τ_0 (elastic response – rule 1). The former depends on the coefficient of friction μ and on the compressive stress f_n perpendicular to the mortar joints.

$$\tau_m = \tau_0 + \mu\,|f_n| \leq \tau'_{max} \quad se\ f_n < 0 \tag{15}$$

$$\tau_m = \tau_0 \quad se\ f_n \geq 0 \tag{16}$$

Figure 19 shows the cyclic analytical shear response of mortar joints, where τ'_{max} represents an upper limit for the shear strength according to analytical and experimental data; somehow, for medium to high values of the compressive strength f_n, the previous equation (15) is not valid. So, the values of μ and τ_0 should be such as to reflect the real strength of the masonry.

When the shear strength is reached, the bond between mortar and brick is destroyed and cracks appear in the affected region. In this phase, one part of the infill panels slides (with respect to the other part) and only the frictional mechanism remains (sliding-rule 2). Consequently the shear strength is given by equation (17), where μ_r is the residual coefficient of friction.

$$\tau_m = \mu_r\,|f_n| \leq \tau'_{max} \quad se\ f_n < 0 \tag{17}$$

$$\tau_m = 0 \quad se\ f_n \geq 0 \tag{18}$$

It is assumed that the unloading and reloading after the bond failure follows a linear relationship. This process can be represented by rule 1, using equation (15). The reloading line increases the shear stress until the shear strength is reached and sliding starts again (Figure 19).

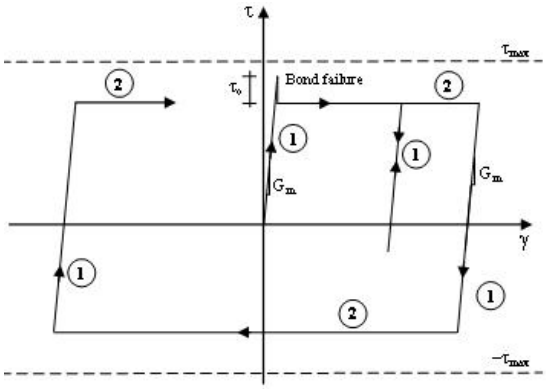

Figure 19 – Analytical response for cyclic shear response of mortar joints

Finally in what refers to the masonry infill panel models, using SAP 2000 [5] and MIDAS/CIVIL [6], it is necessary to define the behavior model specified in such programs as was done by Fardis and Panagiotakos [21] and more recently by Braz-Cesar, Oliveira and Carneiro-Barros [22]. Those models consist in the introduction of equivalent ties which only work in compression.

With the purpose of defining the curve which represents the model, at least three points are necessary in order to obtain it (Figure 20). The first point corresponds to the yielding of material, for the coordinates (f_c,d_c). Then, the next point is associated to maximum force installed in the equivalent tie, for the coordinates (f_m,d_m). In this second segment between first and second point, it is quite visible the occurrence of progressive degradation of stiffness, because the inclination of the segment is smaller when comparing with the last one. That is due to the cracking process that takes place in the panel, leading to a clearly reduction of the stiffness in the structure (Cesar, Oliveira and Barros [22]). Finally, the last point, coincident with the displacement axis, it means the total break down and absence of any resistant capacity in the panel ("collapse"), corresponding to a displacement D_u.

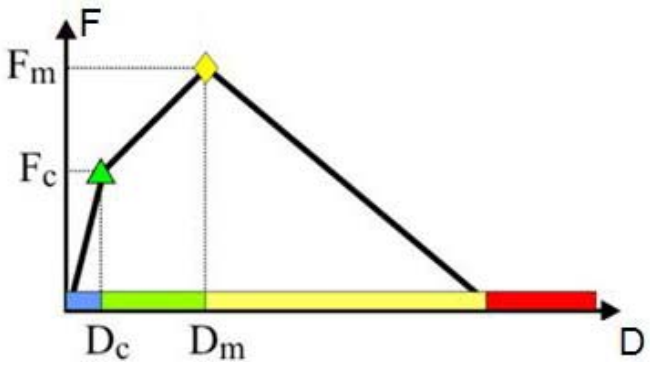

Figure 20 – Masonry infill model introduced in SAP 2000 [5] and MIDAS/CIVIL [6]

After the explanation about the meaning of those points, considered fundamental to the perception of the curve, the following Table 2 presents all the values given to the forces and displacements necessary for the definition of the masonry model.

Table 2 – Values related to the forces and displacements of the masonry model

Equivalent tie behavioral model					
F_c (kN)	D_c (m)	F_m (kN)	D_m (m)	F_u (kN)	D_u (m)
110	0,001	135	0,075	0	0,3

RESULTS

With all the peculiarities on the pushover analysis properly addressed, the final results obtained with the three commercial programs before-mentioned are now presented in this section. The results are in fact the capacity curves of the structure under various load distributions in height, the variation of the maximum basal shear in the structure according to the parametric study and finally the determination of the maximum relative displacement between floors (floor drifts) for the defined load patterns. For steps 1 and 2 (only a single level of structure, for the pushover analysis sequence considered) only the uniform distribution will be addressed because all the three distribution are essentially the same. Furthermore, the influence of masonry panels will only be studied in steps 3 and 4 (since, in office buildings, the first floor is almost entirely glazed). In those analyses, only the results of the last event of the parametric study (beam spans of 7 meters and floor height of 4 meters) will be presented because they will surely give the higher values of the structural response when pushover analysis is carried out.

STEP ONE OF THE PUSHOVER ANALYSIS

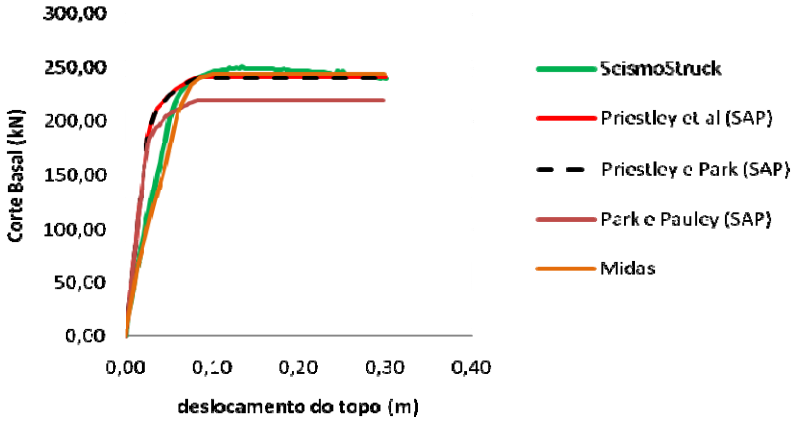

Figure 21 – Capacity curves

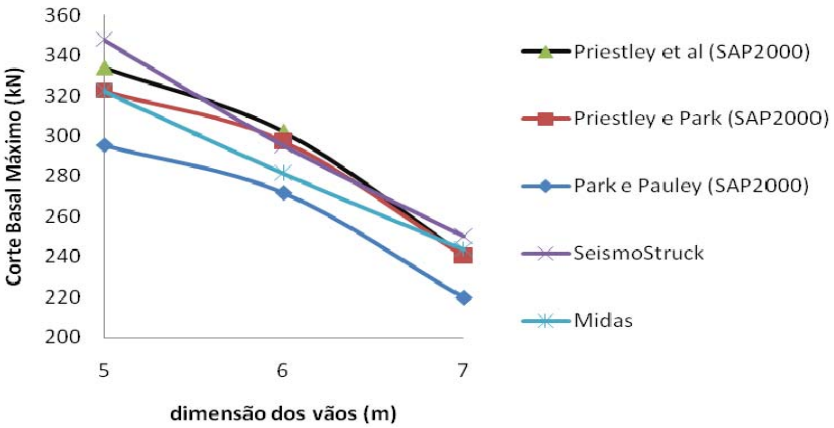

Figure 22 – Maximum base shear variation

STEP TWO OF THE PUSHOVER ANALYSIS

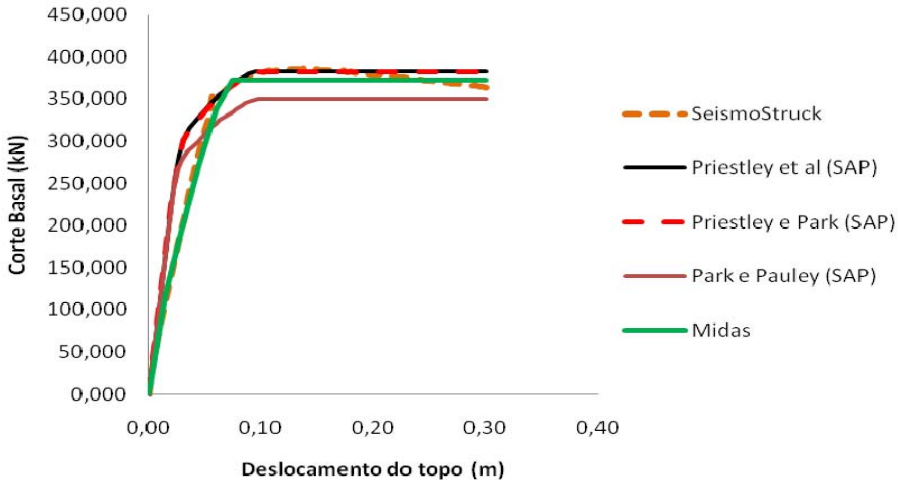

Figure 23 – Capacity curves

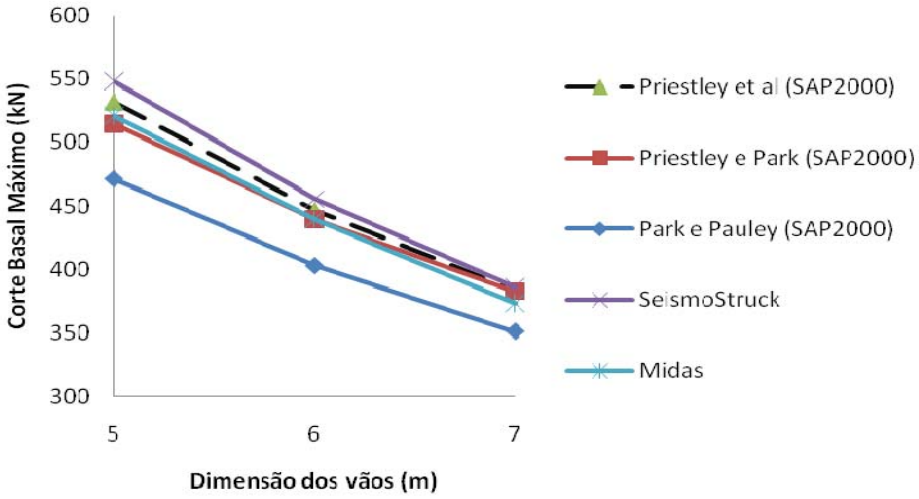

Figure 24 – Maximum base shear variation

STEP THREE OF THE PUSHOVER ANALYSIS

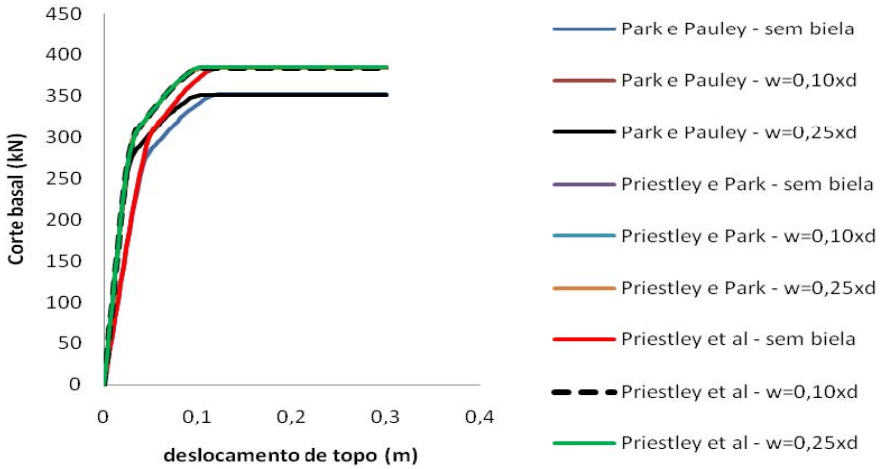

Figure 25 – Capacity curves with uniform load pattern using SAP 2000

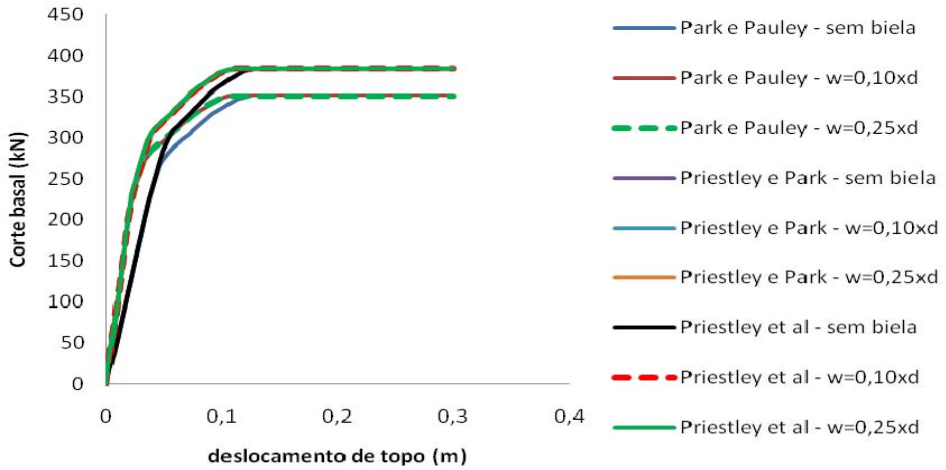

Figure 26 – Capacity curves with modal load pattern using SAP 2000

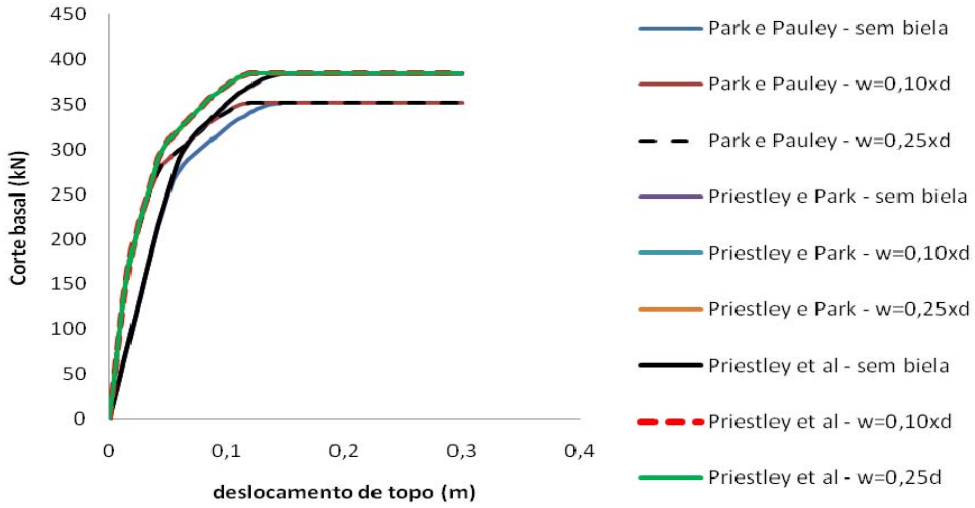

Figure 27 – Capacity curves with triangular load pattern using SAP 2000

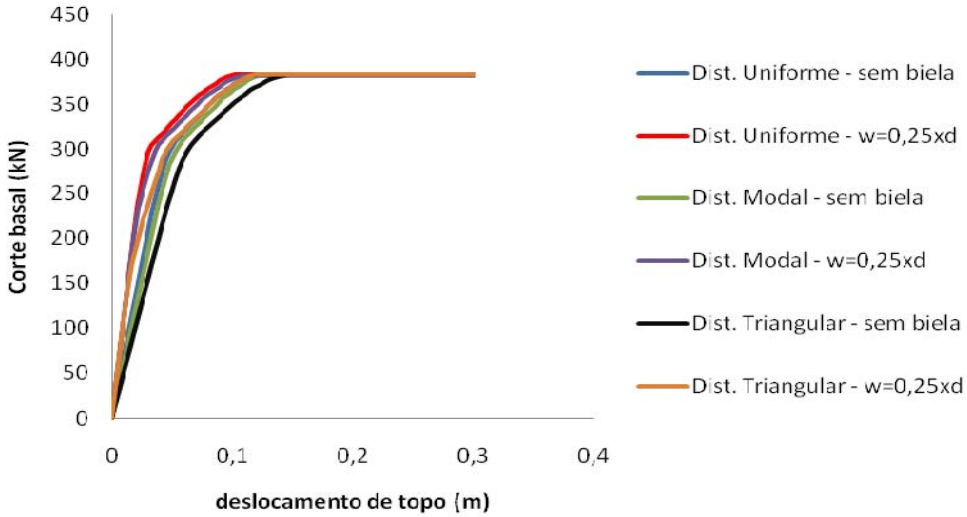

Figure 28 – Capacity curves using proposal of Priestley et al [10] for all types of load pattern distributions (SAP 2000)

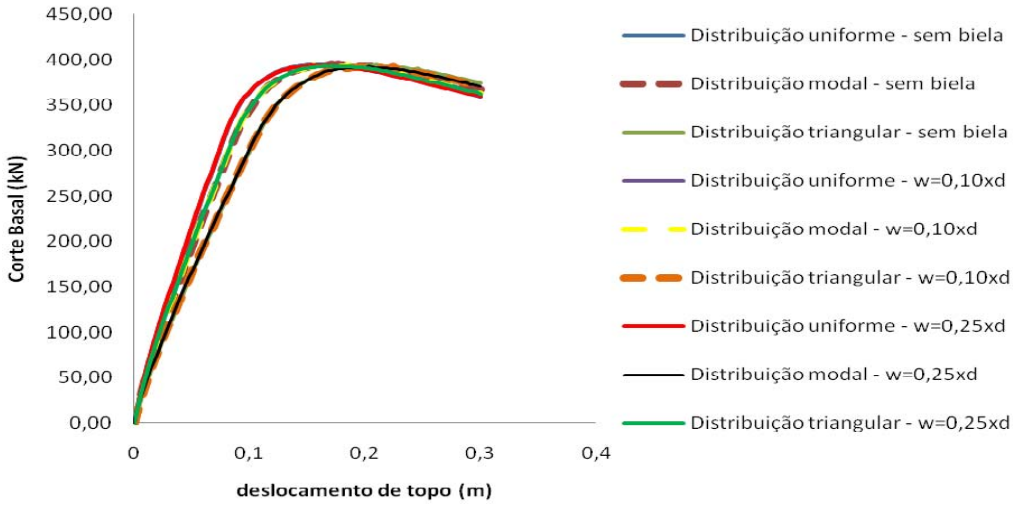

Figure 29 – Capacity curves for all types of load pattern distributions (SeismoStruck)

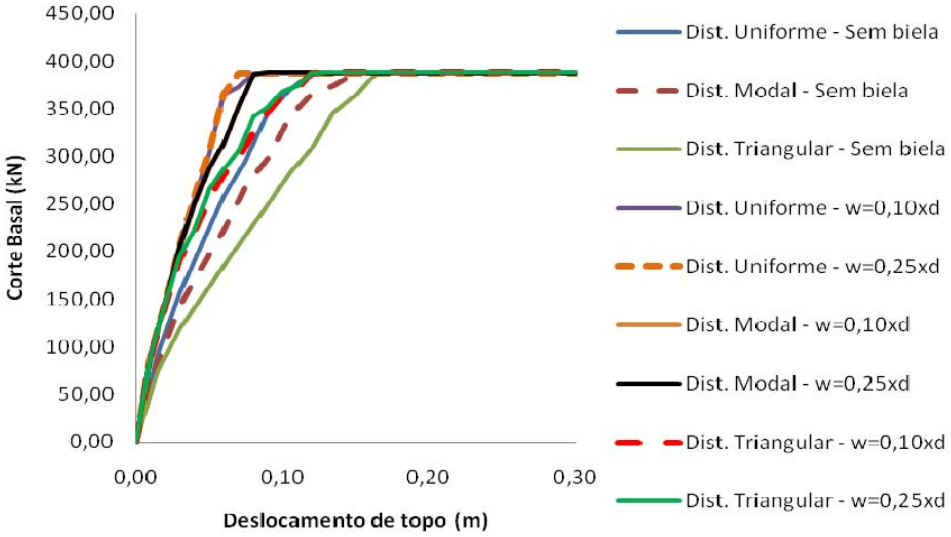

Figure 30 – Capacity curves for all types of load pattern distributions (MIDAS/CIVIL)

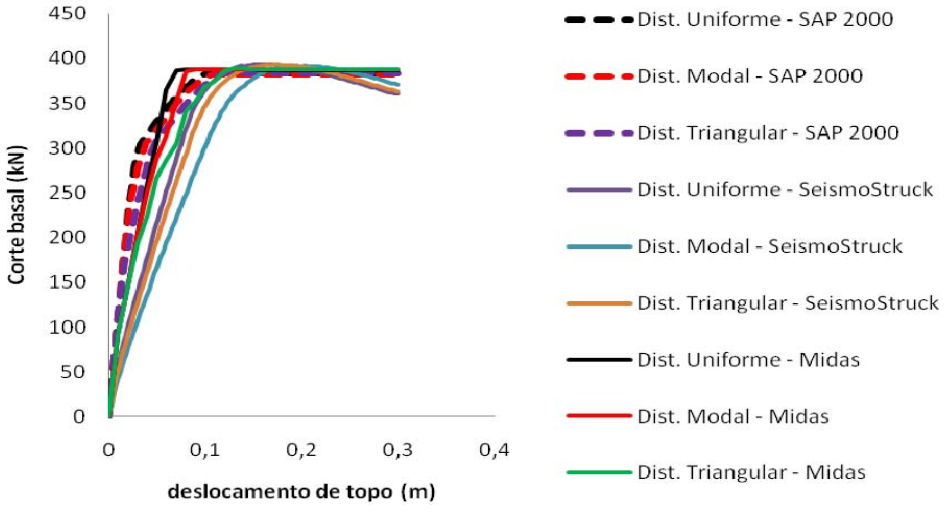

Figure 31 – Comparison of the capacity curves (3 software) for all types of load pattern distributions

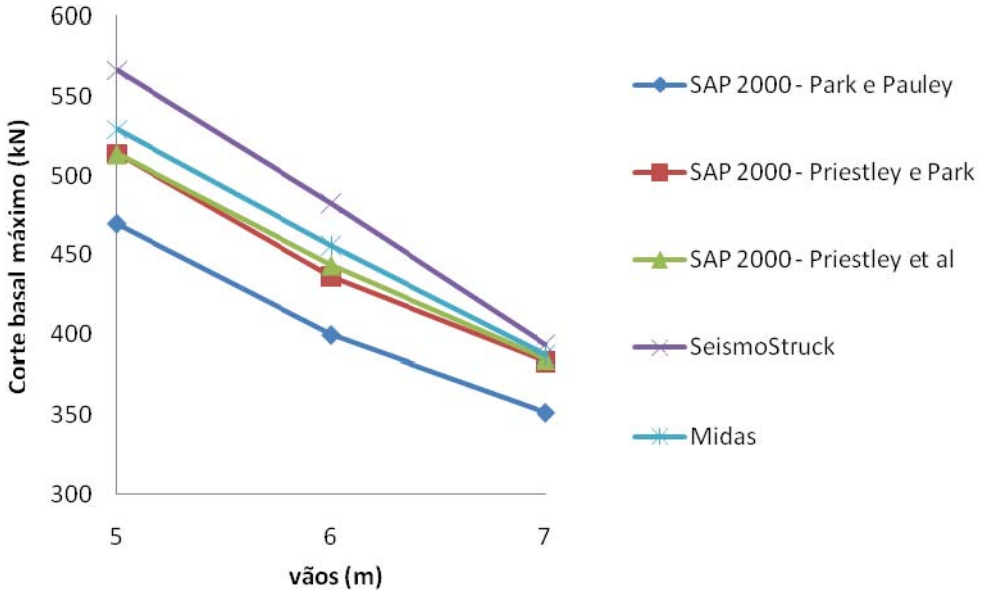

Figure 32 – Variation of the maximum base shear related to an uniform load distribution and considering a tie width of 25% of the diagonal length of the panel

The maximum drifts verified in those analyses are presented bellow, in the following tables. Each table corresponds to different software.

Table 3 - Drifts using the proposal of Priestley et al [10] for all load pattern distributions (SAP 2000)

Case 3			
Uniform distribution			
Storey's	Priestley et al		
	w/ tie	w=0,10xd	W=0,25xd
R/C – 1º Floor	0,2789	0,2922	0,2950
1º Floor – 2º Floor	0,0211	0,0050	0,0050
Modal distribution			
Storey's	Priestley et al		
	w/ tie	w=0,10xd	w=0,25xd
R/C – 1º Floor	0,2724	0,2870	0,2887
1º Floor – 2º Floor	0,0276	0,0125	0,0113
Triangular distribution			
Storey's	Priestley et al		
	w/ tie	w=0,10xd	w=0,25xd
R/C – 1º Floor	0,2550	0,2775	0,2775
1º Floor – 2º Floor	0,0450	0,0225	0,0225

Table 4 - Drifts obtained with SeismoStruck [7] for all load pattern distributions

Case 3			
Uniform distribution			
Storey's	w/ tie	W=0,10xd	w=0,25xd
R/C – 1º Floor	0,12578	0,12622	0,12485
1º Floor – 2º Floor	0,03686	0,03641	0,03778
Modal distribution			
Storey's	w/ tie	w=0,10xd	w=0,25xd
R/C – 1º Floor	0,12914	0,12730	0,12758
1º Floor – 2º Floor	0,04871	0,04753	0,04725
Triangular distribution			
Storey's	w/ tie	W=0,10xd	w=0,25xd
R/C – 1º Floor	0,13646	0,13442	0,13489
1º Floor – 2º Floor	0,0748	0,07383	0,07336

Table 5 – Drifts obtained with MIDAS/CIVIL [6] for all load pattern distributions

Case 3			
Uniform distribution			
Storey's	w/ tie	W=0,10xd	w=0,25xd
R/C – 1º Floor	0,248	0,292	0,293
1º Floor – 2º Floor	0,052	0,008	0,007
Modal distribution			
Storey's	w/ tie	w=0,10xd	w=0,25xd
R/C – 1º Floor	0,241	0,280	0,282
1º Floor – 2º Floor	0,059	0,020	0,018
Triangular distribution			
Storey's	w/ tie	W=0,10xd	w=0,25xd
R/C – 1º Floor	0,191	0,195	0,259
1º Floor – 2º Floor	0,079	0,045	0,041

STEP FOUR OF THE PUSHOVER ANALYSIS

Capacity curves with software SAP 2000 [2]:

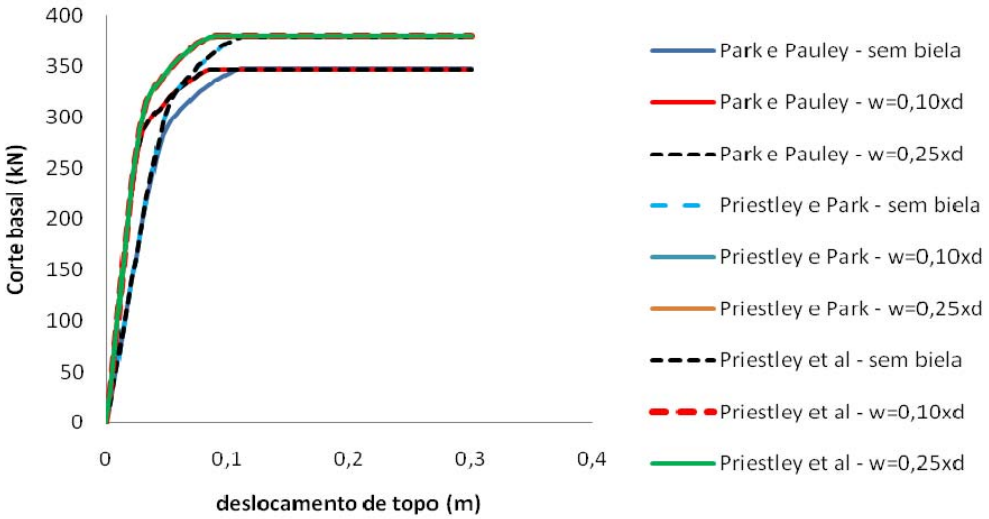

Figure 33 - Capacity curves with uniform load pattern using SAP 2000

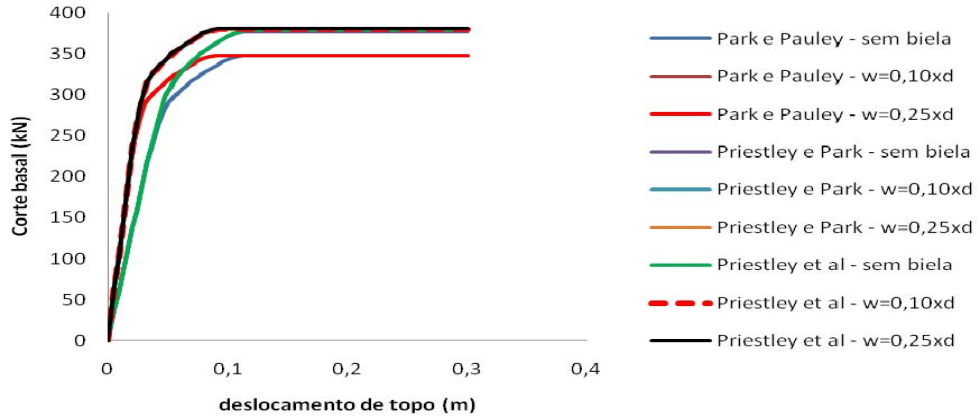

Figure 34 – Capacity curves with modal load pattern using SAP 2000

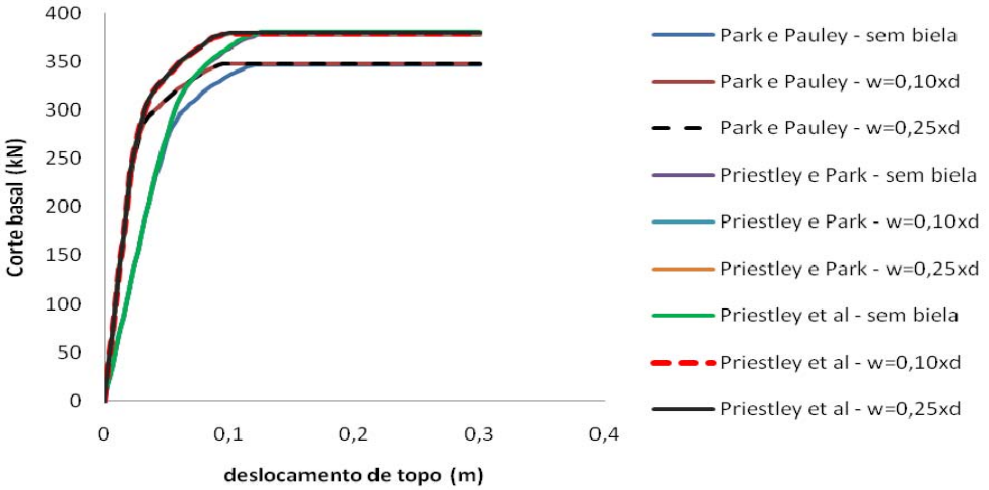

Figure 35 – Capacity curves with triangular load pattern using SAP 2000

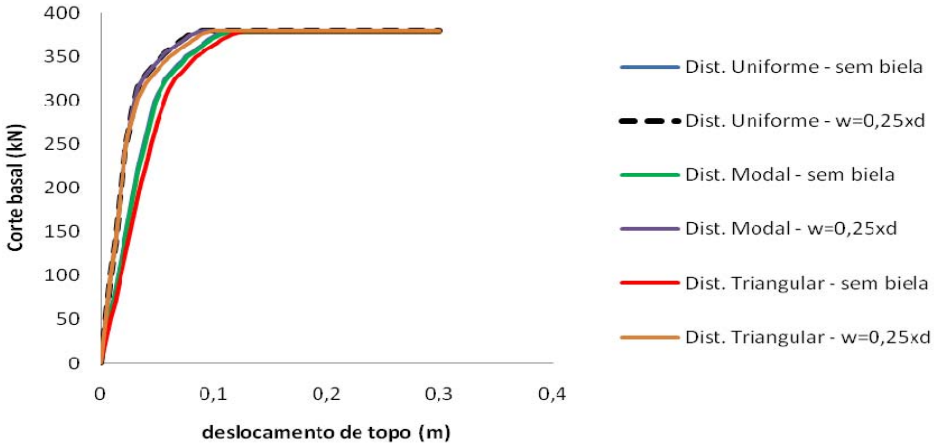

Figure 36 – Capacity curves using proposal of Priestley et al [10] for all types of load pattern distributions

Capacity curves with software SeismoStruck [7]:

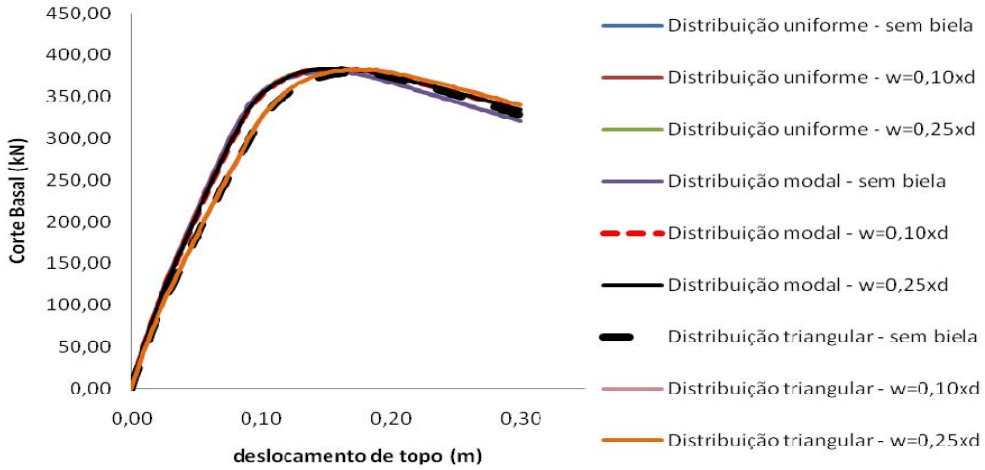

Figure 37 – Capacity curves for all types of load pattern distributions

Capacity curves with software MIDAS/CIVIL [6]:

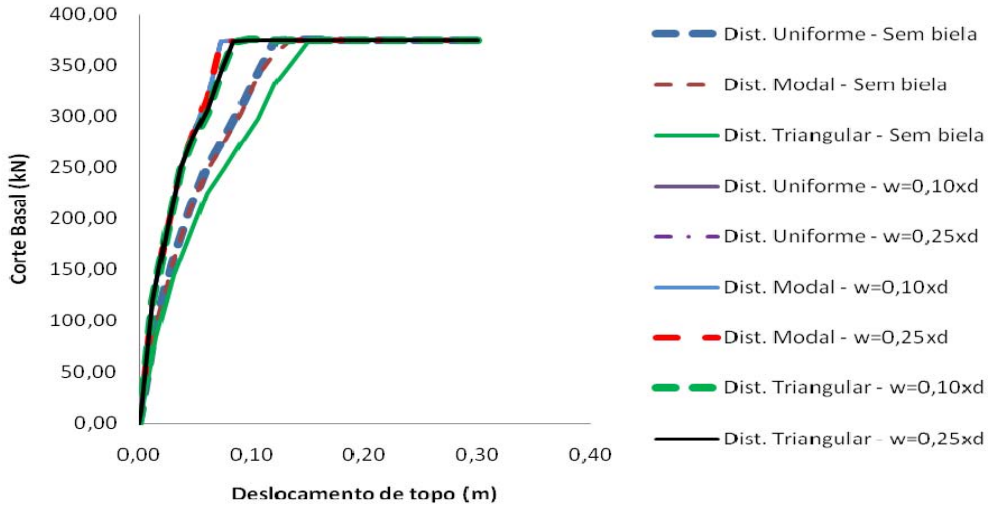

Figure 38 – Capacity curves for all types of load pattern distributions

Comparison of capacity curves obtained from the three software used:

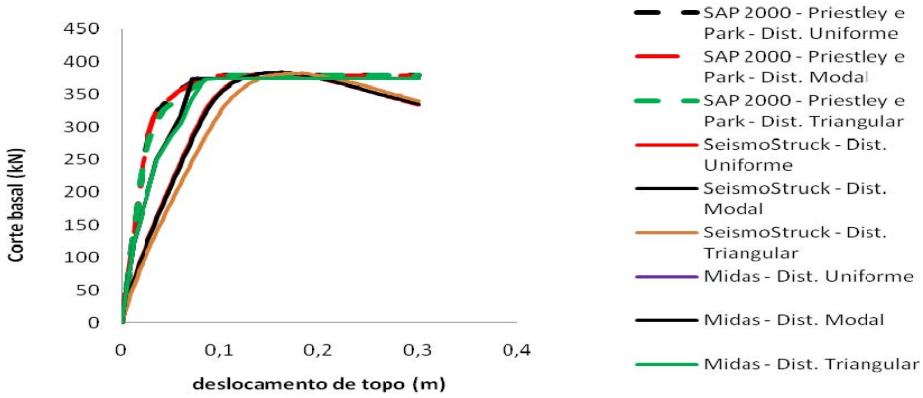

Figure 39 – Comparison of capacity curves obtained with the three software for all types of load distributions

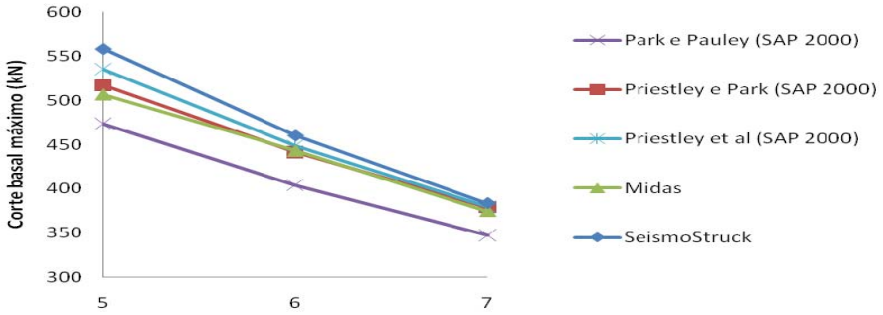

Figure 40 – Variation on the maximum base shear related to an uniform load pattern and considering a tie width of 25% of the diagonal length of the panel

Table 6 - Drifts corresponding to proposal of Priestley et al [10] for all load patterns, using SAP 2000

Case 3			
Uniform distribution			
Storey's	Priestley et al		
	w/ tie	w=0,10xd	w=0,25xd
R/C – 1º Floor	0,2782	0,2990	0,2989
1º Floor – 2º Floor	0,0218	0,0010	0,0011
Modal distribution			
Storey's	Priestley et al		
	w/ tie	w=0,10xd	W=0,25xd
R/C – 1º Floor	0,2771	0,2961	0,2979
1º Floor – 2º Floor	0,0229	0,0027	0,0021
Triangular distribution			
Storey's	Priestley et al		
	w/ tie	w=0,10xd	w=0,25xd
R/C – 1º Floor	0,2675	0,2903	0,2903
1º Floor – 2º Floor	0,0325	0,0097	0,0097

Table 7 - Drifts obtained with SeismoStruck [7] considering all load pattern distributions

Case 3			
Uniform distribution			
Storey's	w/ tie	w=0,10xd	w=0,25xd
R/C – 1º Floor	0,12442	0,12509	0,12545
1º Floor – 2º Floor	0,03817	0,03749	0,03712
Modal distribution			
Storey's	w/ tie	w=0,10xd	w=0,25xd
R/C – 1º Floor	0,12532	0,12613	0,12649
1º Floor – 2º Floor	0,04031	0,03948	0,03912
Triangular distribution			
Storey's	w/ tie	w=0,10xd	w=0,25xd
R/C – 1º Floor	0,1284	0,12345	0,12385
1º Floor – 2º Floor	0,05538	0,05432	0,05391

Table 8 - Drifts obtained with MIDAS/CIVIL [6] considering all load pattern distributions

Case 3			
Uniform distribution			
Storey's	w/ tie	w=0,10xd	w=0,25xd
R/C – 1º Floor	0,260	0,296	0,297
1º Floor – 2º Floor	0,040	0,004	0,003
Modal distribution			
Storey's	w/ tie	w=0,10xd	w=0,25xd
R/C – 1º Floor	0,258	0,295	0,295
1º Floor – 2º Floor	0,042	0,005	0,005
Triangular distribution			
Storey's	w/ tie	w=0,10xd	w=0,25xd
R/C – 1º Floor	0,237	0,285	0,287
1º Floor – 2º Floor	0,063	0,015	0,013

CONCLUSIONS

The primary objective of this article is the presentation of a simplified methodology (pushover analysis) giving the response of a RC office frame under seismic action, considering non-linear effects. To achieve this, four evolutionary steps were studied in detail as far as the final stage of frame is reached with two spans and two storey's. Varying the values of the spans and of the inter-storey height, a parametric study is performed from which some conclusions can be taken about the parameters influence on the basal shear of the structure. The pushover analyses were performed using three software: two based on concentrated plastic hinges (SAP 2000 [5] and MIDAS/CIVIL [6]); and another based on distributed hinges (SeismoStruck [7]).

Confronting the capacity curves obtained by all of them, it was found that the final level of all the pushover curves – except the joint proposal from Park and Paulay [8] made in SAP 2000 [5] – become close together as the parametric study progresses.

On the capacity curves obtained by the MIDAS/CIVIL [6], it was observed that the ascending branch follows closely the one obtained with the SeismoStruck [7]. Moreover the final branch of the curves, which is the maximum basal shear of the structure, is very near to the one obtained with SeismoStruck [7] and even with SAP 2000 [5] by the joint proposals of Park et al [9] and Priestley et al [10]. It can also be concluded that the yielding of the RC frame sections occurs earlier for the joint proposals made in the SAP 2000 [5] in comparison to MIDAS/CIVIL [6] and SeismoStruck [7].

Moreover, for the curves obtained in steps 3 and 4, it is clear that in the case of considering equivalent tie widths of 10% and 25% of the diagonal length of the panel, there was not a major difference in the capacity curves obtained. Although, considering the assumptions of absence of tie and a tie with a thickness equal to 25% of the diagonal length of the panel, there is a certain difference in the curves (with the ascending branch slightly different). With the inclusion of the ties in the model, there is greater stiffness in the structure so that the top displacements are smaller.

There is thus a constant reduction of top displacement, for the same basal shear value. However, all the curves converge to the same maximum basal shear value.

In what refers to the load patterns, it appears that by adopting the triangular distribution, a greater discrepancy in the curves under the various proposals is surely seen, which is very evident in the curves obtained by MIDAS/CIVIL [6]. Moreover, the clearly seen bundle of curves represented is due to a greater parametric variability. It was also observed that the curves obtained by uniform and modal distribution are close enough comparing to the triangular one.

Finally, also the maximum inter-storey displacements were calculated, showing that between the ground floor and 1st floor the drifts are more significant in SAP2000 [5] and MIDAS/CIVIL [6], while the relative displacements between 1st and 2nd floors are higher in SeismoStruck [7]. This difference observed, more specifically between the last two floors, can be justified based on the behavioral models embedded in SeismoStruck [7] in which two modes of failure are included: compressive failure of the equivalent tie and shear failure. In other words, the redistribution of stress in view of the possible modes of failure included in this program, and their interaction, leads to a resistance in rupture with higher values compared to SAP2000 [5] and MIDAS/CIVIL [6]; therefore, also the drifts are higher in case of using SeismoStruck [7].

Disregarding the influence of masonry panels on the 2nd floor, it appears that the relative displacements between the last floors are higher because there is not enough stiffness in the structure like in the case of equivalent ties consideration. Moreover, the modal and uniform distributions are indeed the ones that become closest, which is evident in the results obtained by SeismoStruck [7]. For buildings with 1 or 2 levels, the modal and triangular distributions are not very similar, which no longer happens in multi-storey regular buildings. In this case, the modal and triangular distributions become very close because the fundamental mode controls the response of the structure.

ACKNOWLEDGEMENTS

This work reports some research on pushover analyses of reinforced concrete frames developed under the R&D Eurocores Project COVICOCEPAD within the S3T Program, approved independently by European Science Foundation (ESF, Strasbourg). It is financially supported by portuguese "FCT – Fundação para a Ciência e a Tecnologia" (Lisbon – Portugal) under *Programa Operacional Ciência e Inovação 2010* (POCI 2010) of the *III Quadro Comunitário de Apoio* funded by FEDER, and also by italian "CNR – Centro Nazionale della Ricerca" (Rome – Italy), under the EC Sixth Framework Program. This alternative nonlinear static analysis of frames under earthquakes is important in the context of the project, since it constitutes a simplified alternative to ascertain building capacity even for buildings equipped with vibration control devices.

Special thanks are also due to Prof. Rui Pinho at Rose School of the University of Pavia, for providing the latest version of SeismoStruck and for the rich exchange of information between our institutions.

REFERENCES

[1] Fajfar, P., Fischinger, M. "N2 – A method for non-linear seismic analysis of regular buildings". *Proceedings* of the 9th World Conference in Earthquake Engineering, 1988, Vol.5, 111-116, Tokyo- Kyoto, Japan.

[2] Eurocode 8: Design of structures for earthquake resistance; Part 1: General Rules, seismic actions and rules for buildings; CEN, Brussels, 2003.

[3] Cesar, M.B. and R.C. Barros, "Estudo Preliminar sobre o Desempenho Sísmico de Pórticos Metálicos Contraventados a partir de Análises Estáticas Não-Lineares (Pushover)"; *Proceedings* of 'Métodos Numéricos e Computacionais em Engenharia CMNE 2007 e XXVIII CILAMCE', Congresso Ibero Latino-Americano sobre Métodos Computacionais em Engenharia, FEUP, Porto, 13-15 Junho 2007; CMNE/CILAMCE 2007, Paper 1184 – pp. 1-18; Edts: A. Rodriguez-Ferran, Javier Olivier, Paulo R.M. Lyra, José L.D. Alves; APMTAC / SEMNI, 2007.

[4] Cesar, M.B. and R.C. Barros, "Seismic Performance of Metallic Braced Frames by Pushover Analyses", *Computational Methods in Structural Dynamics and Earthquake Engineering* (COMPDYN 2009), M. Papadrakakis, N.D. Lagaros, M. Fragiadakis (eds.), Rhodes, Greece, 22–24 June 2009 (*in press*).

[5] Computers & Structures Inc.; "SAP2000 v10.0.1 – Structural Analysis Program". Berkeley, California, U.S.A., 2005.

[6] MIDASIT - MIDAS/CIVIL, "General purpose analysis and optimal design system for civil structures", MIDAS Information Technology Co, Ltd., Korea, 2005.

[7] SeismoSoft SeismoStruck, "A Computer Program for Static and Dynamic Nonlinear Analysis of Framed Structures". Available online at: http://www.seismosoft.com; 2006.

[8] Park, R. and T. Paulay, *Reinforced Concrete Structures*. John Wiley & Sons Inc., New York, 1975.

[9] Park, R., Priestley, M.J.N., and W.D. Gill; "Ductility of square-confined concrete columns", Journal of the Structural Division, ASCE, Vol. 108, No. ST 4, pp. 929-950, 1982.

[10] Priestley, M.J.N., Seible, F. and G.M.S. Calvi, *Seismic design and retrofit of bridges*. John Wiley & Sons Inc., New York, 1996.

[11] Fagus, Fagus-5: Version 1.22.0 Build 275, Cubus AG, Zurïch, 2000-2006.

[12] Eurocódigo 2: Projecto de estruturas de betão; Parte 1-1: Regras gerais e regras para edifícios. Comité Europeu de Normalização, Brussels, 2004.

[13] Moehle, J. and S.A. Mahin, "Observations on the behaviour of reinforced concrete buildings during earthquakes", ACI publication SP-127, Earthquake-Resistant Concrete Structures: Inelastic Response and Design, S.K. Ghost (ed.), USA, 1991.

[14] Carneiro Barros, R. and Ricardo F. Almeida, "Pushover Analysis of Asymmetric Three-Dimensional Building Frames", *Journal of Civil Engineering and Management*, Vol. XI, Number 1, pp. 3-12, Vilnius, Lithuania, 2005.

[15] Polyakov, S. V., *Masonry in framed building: an investigation into the strength and stiffness of masonry infilling*, Moscow, 1957.

[16] Stafford Smith, B. and C. Carter, "A method of analysis for infilled frames", *Proceedings of the Institution of Civil Engineers*, Vol. 44, 1969.

[17] Riddington, J. R. and B. Stafford Smith, "Analysis of infilled frames subject to racking with design recommendations", *The Structural Engineer*, Vol. 55, Nº 6, 1977.

[18] Paulay, T. and M. Priestley, *Seismic Design of Reinforced Concrete and Masonry Buildings*, John Wiley & Sons, 1992.

[19] Crisafulli F.J., *Seismic Behaviour of Reinforced Concrete Structures with Masonry Infills*, PhD Thesis, University of Canterbury, New Zealand, 1997.

[20] Blandon, C.A., *Implementation of an Infill Masonry Model for Seismic Assessment of Existing Buildings*, Individual Study, European School for Advanced Studies in Reduction of Seismic Risk (ROSE School), Pavia, Italy, 2005.

[21] Fardis, M.N. and T.B. Panagiotakos, "Seismic design and response of bare and masonry-infilled reinforced concrete buildings – Part II: Infilled structures", *Journal of Earthquake Engineering*, Vol. I, No 3, 475-503, 1997.

[22] Braz-Cesar, M., Oliveira, D.V. and R. Carneiro-Barros, "Numerical Validation of the Experimental Cyclic Response of RC Frames", Chapter 12 in the book *Trends in Computational Structures Technology*, Edited by: B.H.V. Topping, Saxe-Coburg Publications, ISBN 978-1-874672-39-5, pp. 267-291, Stirlingshire, Scotland, 2008.